JOURNAL OF VIROLOGY, Sept. 1993, p. 5163–5174
0022-538X/93/095163-12$02.00/0

Vol. 67, No. 9

Assembly and Composition of Intracellular Particles Formed by Moloney Murine Leukemia Virus

MARK HANSEN, LAURA JELINEK, RUSSELL S. JONES, JENNY STEGEMAN-OLSEN, AND ERIC BARKLIS*

Vollum Institute for Advanced Biomedical Research, Department of Microbiology and Immunology, and Department of Pathology, Oregon Health Sciences University, Portland, Oregon 97201

Received 26 August 1992/Accepted 18 May 1993

Assembly of type C retroviruses such as Moloney murine leukemia virus (M-MuLV) ordinarily occurs at the plasma membranes of infected cells and absolutely requires the particle core precursor protein, $Pr65^{gag}$. Previously we have shown that $Pr65^{gag}$ is membrane associated and that at least a portion of intracellular $Pr65^{gag}$ protein appears to be routed to the plasma membrane by a vesicular transport pathway. Here we show that intracellular particle formation can occur in M-MuLV-infected cells. M-MuLV immature particles were observed by electron microscopy budding into and within rough endoplasmic reticulum, Golgi, and vacuolar compartments. Biochemical fractionation studies indicated that intracellular $Pr65^{gag}$ was present in nonionic detergent-resistant complexes of greater than 150S. Additionally, viral RNA and polymerase functions appeared to be associated with intracellular particles, as were Gag–β-galactosidase fusion proteins which have the capacity to be incorporated into virions. Immature intracellular particles in postnuclear lysates could be proteolytically processed in vitro to mature forms, while extracellular immature M-MuLV particles remained immature as long as 10 h during incubations. The occurrence of M-MuLV-derived intracellular particles demonstrates that $Pr65^{gag}$ can associate with intracellular membranes and indicates that if a plasma membrane $Pr65^{gag}$ receptor exists, it also can be found in other membrane compartments. These results support the hypothesis that intracellular particles may serve as a virus reservior during in vivo infections.

To assemble an infectious retrovirus particle, several components must colocalize and assemble in an ordered manner. The major viral structural protein (Gag) is central to the assembly process (40). The Gag protein is cotranslationally myristylated at its amino terminus (17), and acylation of the matrix domain is required for membrane association and assembly (30). There appear to be 5,000 to 10,000 precursor Gag molecules in each virus particle (40), which oligomerize to form the viral core. In the case of Moloney murine leukemia virus (M-MuLV) and other retroviruses, expression of the Gag protein alone produces noninfectious virus particles (15, 21, 37). The M-MuLV Gag protein is synthesized as a 65-kDa precursor polypeptide ($Pr65^{gag}$), which is cleaved proteolytically into the four mature Gag proteins: matrix (MA), p12, capsid (CA), and nucleocapsid (NC). The protease responsible for this cleavage is encoded by the virus, and the processing of $Pr65^{gag}$ is required for infectivity: M-MuLV protease (PR) mutants assemble to produce noninfectious virus particles that bud in an apparently normal fashion and contain strictly $Pr65^{gag}$ (19).

In addition to Gag, three other components normally are assembled into infectious M-MuLV virions, and each may be directed by the $Pr65^{gag}$ protein. The matrix domain of Gag has been postulated to associate with the transmembrane envelope (Env) protein, which travels to the plasma membrane by vesicular transport (2, 40). The M-MuLV envelope protein complex is synthesized as a precursor ($Pr80^{env}$) which is cleaved to form a receptor binding (RB) domain (gp70) associated with a transmembrane (TM) anchor domain (p15E). Assembly of infectious virions also mandates inclusion of the retroviral genome, consisting of two strands of RNA which may be bound by the carboxy-terminal Gag nucleocapsid domain (14). The other components are the products of the *pol* gene and include PR, reverse transcriptase (RT), and integrase (IN) activities. The Pol proteins depend on Gag protein domains during assembly as Pol, and Pol proteins appear to be incorporated into virions initially as Gag-Pol fusion proteins.

Assembly of type C retroviruses, such as M-MuLV, is thought to occur at the plasma membrane, following the cytoplasmic transport of Gag precursor monomers (2). Electron micrographs have shown assembling and budding virus particles at the plasma membrane (36, 40, 41), and assembly of temperature-sensitive mutants can occur at the plasma membrane within minutes of shifting to the permissive temperature (41). This process is distinct from assembly of type D retroviruses, in which virus cores are formed intracytoplasmically and are delivered to the plasma membrane (32–34). However, in either case, preferential assembly at or association with the plasma membrane appears essential and could be mediated either by an inhibition of assembly at internal membranes or by specific binding to a plasma membrane receptor. Precedent for the latter mechanism has been provided by characterization of a membrane receptor specific for the myristylated Src protein (31).

During our investigations on M-MuLV Gag–β-galactosidase (GBG) fusion proteins, we observed fusion proteins that were released from cells in both viral and nonviral forms but were surprised to observe fusion proteins which localized to intracellular membranes (18), reminiscent of mutant secretory proteins trapped in the vesicular transport pathway (12, 35). That some percentage of Gag proteins might be transported to the cell surface via vesicles was suggested by monensin inhibition of M-MuLV particle assembly (16). Consistent with these results were electron microscope (EM) observations of intracisternal particles formed during occasional avian, murine, and human retrovirus infections

* Corresponding author.

(40). In our efforts to corroborate previous ultrastructural studies, we examined several cell types expressing M-MuLV and have observed virus particles within intracellular membrane compartments. Biochemical analyses support our EM studies, showing that intracellular particles are not endogenous intracisternal type A particles and indicating that a proportion of the intracellular M-MuLV Gag precursor protein is present in a detergent-resistant particle form. These intracellular MuLV particles appear to contain both viral RNA and *pol* gene products. Our observations have specific implications with regard to retrovirus infections and Gag protein transport and assembly mechanisms.

MATERIALS AND METHODS

Cell culture. NIH 3T3, Psi2 (23), and PA317 (25) cells were grown as described previously (1). 3T3 and Psi2 cells expressing recombinant retrovirus constructs were obtained by infection and selection (18). The TR291F cell line, expressing an M-MuLV PR mutant, was the kind gift of Alan Rein (19). NIH 3T3 cells expressing infectious M-MuLV were derived by chronic infection with M-MuLV derived from pMOV9 or Sup1 (29).

Viral constructs. BAG, a retroviral vector which expresses neomycin phosphotransferase and β-galactosidase proteins, was the kind gift of Connie Cepko (6). GBG1560 and GBG 2051 are retroviral vectors which express GBG fusion proteins which are poorly (GBG1560) or efficiently (GBG2051) incorporated into retrovirus particles (18). MP10 is a neomycin-transducing retrovirus described previously (1).

Immunofluorescence. Indirect immunofluorescence of M-MuLV Gag protein was performed by standard methods (18). The primary antibody was a tissue culture supernatant of rat hybridoma cells 34 (kindly provided by Bruce Chesebro [7]) used at a 1:3 dilution for detection of M-MuLV matrix $p15^{gag}$ protein. The secondary antibody was rhodamine-conjugated anti-mouse immunoglobulin G antibody (TAGO) used at a 1:100 dilution. After the final washes with Dulbecco's modified Eagle's medium supplemented with 10% calf serum, penicillin, streptomycin, and *N*-2-hydroxyethylpiperazine-*N'*-2-ethanesulfonic acid (HEPES) buffer solution (GIBCO BRL), coverslips were washed three times for 5 min each time in phosphate-buffered saline (PBS) and mounted in 50% glycerol in PBS. Cells were viewed with a standard rhodamine filter.

EM. Confluent 10-cm plates of cells were prepared for analysis by decanting the supernatant and fixing the cells for 5 min at 25°C in a fixative of 1.5% glutaraldehyde–1.5% paraformaldehyde in 100 mM sodium cacodylate buffer (pH 7.4). The fixative was decanted, fresh fixative was added, and the cells were maintained at 4°C for 1 h. Cells then were scraped off the petri dishes with a rubber policeman and pelleted. The fixative was removed, and cells were gently resuspended in 0.1 M sodium cacodylate buffer (pH 7.4) for 25 min at 25°C, after which cells were pelleted and then resuspended in 6% bovine serum albumin (BSA) in 0.1 M sodium cacodylate buffer (pH 7.4) for 5 min. Cells were pelleted, and all but 4 mm of overlaying buffer was removed. Fixative was carefully layered above the BSA-buffer solution, and the sample was left overnight at 4°C. This procedure cross-links the BSA and gelatinizes the sample so that it is removed from the centrifuge tube as a solid block that is sectioned into 2-mm cubes for processing. The tissue was washed in 0.1 M sodium cacodylate buffer (pH 7.4) for 25 min at 25°C and then postfixed in 2% OsO_4 for 90 min at 25°C. The samples were dehydrated through graded ethanols, infiltrated with toluene, and infiltrated and embedded in Epon 812. Ultrathin sections were stained with uranyl acetate and lead citrate and then examined on a Philips EM 301 transmission electron microscope (Philips Electronic Instruments, Inc.). To tabulate intracellular particle localization, 22 Psi2 and 22 M-MuLV-infected 3T3 cells were extensively examined for virus particle content. Cells were chosen solely by the criterion that they lay fully within one grid sector. Intracellular particles were distinguished as to whether they were within vacuoles, vesicles, rough endoplasmic reticulum (RER), or Golgi bodies. In each compartment, the number of budding virions was enumerated.

Subcellular fractionation. Typically, three 10-cm-diameter plates of confluent cells were washed twice, pelleted in PBS, and resuspended in 1 ml of Dounce buffer (20 mM HEPES [pH 7.4], 100 mM KCl, 85 mM sucrose, 100 μM EGTA). The cells were lysed by Dounce homogenization 200 times in a 2-ml Wheaton Dounce homogenizer, using the type A (tight) pestle. Whole cell lysates were spun for 5 min at 5,000 × *g* (8,500 rpm on an Eppendorf Microfuge) at 4°C. Postnuclear supernatant (PNS) was collected and either treated or not treated with Triton X-100 to a final concentration of 0.5%. Treated or untreated PNS was spun at 201,000 × *g* (55,000 rpm on a Beckman TLS-55 rotor) for 15 min at 4°C. Second supernatants (S2) and second pellets (P2) were resuspended with either electrophoresis sample buffer or TSE (10 mM Tris HCl [pH 7.4], 100 mM NaCl, 1 mM EDTA), depending on the experiment. In experiments testing the effects of salt on fractionation patterns, 500 mM NaCl was substituted for Triton X-100, giving a final NaCl concentration of 600 mM in these samples. Alternatively, Triton X-100-treated P2 (Triton-P2) pellets were resuspended in Dounce buffer by Dounce homogenization an additional 200 times, mock treated or treated with 500 mM NaCl as described above, and recentrifuged to obtain third supernatants (S3) and pellets (P3) for analysis as described above. For proteolysis time course studies of $Pr65^{gag}$, Psi2 PNS prepared as described above but also containing protease inhibitors (0.1 mM phenylmethylsulfonyl fluoride, leupeptin [5 μg/ml], pepstatin A [2.5 μg/ml], and benzamidine [2 μg/ml]) or medium supernatants from Psi2 cells were incubated at 37°C for the times indicated prior to electrophoresis. As a control for intracellular proteolysis experiments, PNS from the M-MuLV PR-deficient cell line TR291F (19) was used, but in this case, protease inhibitors were omitted.

Concentration of virus particles. Supernatants collected from cells grown to confluency on 15-cm-diameter plates were layered on sucrose step gradients consisting of 3.5 ml of 20% sucrose and 2.5 ml of 60% sucrose in TSE. Samples were centrifuged at 83,000 × *g* (25,000 rpm on an SW28 rotor) for 60 min at 4°C. The 20%/60% interface from six tubes collected in a total volume of 6 ml was diluted by addition of 5 ml of TSE and layered onto a 2-ml 60% sucrose cushion (in TSE) and centrifuged at 151,000 × *g* (SW41 rotor at 35,000 rpm) at 4°C for 75 min. The final interface was collected in 1 ml and frozen at −80°C in aliquots.

Enzymatic assays. Protein quantification was done by the method of Bradford (4), using Bio-Rad reagent and the microassay procedure. β-Galactosidase assays were performed by the method of Norton and Coffin (26). Galactosyltransferase assays were a modified version of Bretz et al. (5), while cytochrome oxidase assays were performed by the method of Omura et al. (27).

Immunoblotting. Samples for immunoblot analysis were prepared in electrophoresis sample buffer (without dithiothreitol) and applied to 7.5 or 10% Laemmli sodium dodecyl

sulfate (SDS)-polyacrylamide protein gels (20) and run at 35 mA. Proteins were transferred to a nitrocellulose membrane (Schleicher & Schuell) on a Hoefer electroblotter at 4°C and 0.15 A overnight, after which membranes were blocked at 25°C in 3% gelatin (Bio-Rad) in TBST (20 mM Tris HCl [pH 7.6], 150 mM NaCl, 0.05% Tween 20 [Bio-Rad]) prior to antibody binding steps. Primary antibody treatments for 30 min at 25°C in 1% gelatin in TBST were with a goat anti-feline leukemia virus gp71 antibody (1:1,500 dilution), tissue culture supernatants of rat hybridoma cells 548 and R187 (from B. Chesebro) used at 1:4 dilutions for immunodetection of $p12^{gag}$ and $p30^{gag}$ proteins, or a rabbit anti-human placental alkaline phosphatase (PLAP) antibody (DAKO), at a 1:1,000 dilution (22). After three 10-min TBST washes, immunodetection was performed with a 1:100 dilution of alkaline phosphatase anti-immunoglobulin G conjugates (Promega anti-mouse; Boehringer Mannheim Biochemicals anti-goat and anti-rabbit). After the secondary antibody binding for 30 min at 25°C in 1% gelatin in TBST, the membranes were washed three times in TBST for 10 min each time and then incubated in 20 ml of a color reaction solution of 0.33 mg of Nitro Blue Tetrazolium, 0.17 mg of 5-bromo-4-chloro-3 indolyl phosphate, 100 mM Tris hydrochloride (pH 9.5), 100 mM NaCl, and 5 mM $MgCl_2$ until bands appeared.

RNase protection. Total cellular RNA was isolated by collecting cells in 1 ml of 6 M guanidium thiocyanate–25 mM sodium citrate (pH 7.0)–0.5% Sarkosyl–100 mM β-mercaptoethanol per 10-cm plate and pelleting through a cushion (2 ml of 6.2 M cesium chloride–100 mM EDTA [pH 7] per 3 ml of lysate) for 18 h at 115,000 × *g* (35,000 rpm on an SW 50.1 rotor [8]). Pellets were washed with 70% ethanol, dried, and resuspended in 10 mM Tris (pH 7.4)–1 mM EDTA. Membrane-associated RNA was isolated from cell lysates (PNS), which were untreated or treated with 0.5% Triton X-100. Samples were centrifuged at 201,000 × *g* for 15 min at 4°C. The pellets were rinsed in 10 mM Tris (pH 7.4)–100 mM NaCl–1 mM EDTA, suspended in 200 μl of 10 mM Tris (pH 7.4)–25 mM EDTA–50 mM NaCl containing 10 μg of yeast tRNA, extracted twice with phenol-chloroform (1:1) and twice with chloroform, and ethanol precipitated. For RNase protection assays, 10-μg samples of tRNA, membrane-associated RNA, or total cellular RNA were precipitated and dried just prior to annealing reactions.

Riboprobe transcription templates were prepared in the following manner. A 250-bp *Rsa*I fragment of ribosomal protein L3 (rpL3 [28]) was inserted into the *Sma*I site of Bluescript −SK. This construct was linearized with *Bam*HI and transcribed from the T7 promoter, resulting in a runoff transcript approximately 250 nucleotides long. A neomycin (*neo*) probe was constructed by cloning a 542-bp *Pst*I-*Hin*dIII fragment from the *neo* gene into the Bluescript -KS cloning vector. This plasmid was linearized at the *Bgl*II site and transcribed from the T7 promoter, resulting in a runoff transcript approximately 260 nucleotides long.

Probe transcription reaction mixtures contained 1 μg of linearized plasmid, 3 U of T7 polymerase, 100 μCi of [^{32}P]rGTP (specific activity of 600 Ci/mmol), 500 μM each of the other ribonucleotides, 40 mM Tris (pH 7.9), 10 mM NaCl, 6 mM $MgCl_2$, 2 mM spermidine, and 1 mM dithiothreitol and RNasIn (40 U; Promega). Reaction incubations were for 1 h at 37°C and were terminated by phenol-chloroform extraction after the addition of 10 μg of tRNA, 120 U of RNasIn (Promega), and sodium acetate (pH 7.6) to a final concentration of 300 mM. Ethanol-precipitated probes then were purified away from free nucleotides and partial synthesis products by denaturing DNA acrylamide gel electrophoresis. After elution from the gel by a 50°C incubation with 1 M ammonium acetate (pH 7.4)–0.1% SDS–1 mM EDTA, probes were extracted twice, precipitated, and suspended in 20 μl of water.

Annealing reactions combined 1×10^5 to 5×10^5 cpm of probe with the precipitated RNA samples in 80% formamide–400 mM NaCl–40 mM piperazine-*N*,*N*′-bis(2-ethanesulfonic acid) (PIPES; pH 6.4). These samples were denatured at 85°C for 5 min and incubated at 37°C overnight. Unbound probe was eliminated by incubation at 30°C for 30 min in 350 μl of 300 mM NaCl–10 mM Tris (pH 7.5)–5 mM EDTA–15 μg of RNase A–1.4 μg of RNase T_1. This reaction was terminated by incubation at 37°C for 15 min with 50 μg of proteinase K (Boehringer Mannheim) and 0.1% SDS. The protected probe was extracted after addition of 20 μg of tRNA and ethanol precipitated. The pellet was rinsed, dried, and suspended in 5 μl of sequence loading dye. Samples were denatured and run on a 6% acrylamide sequencing gel that was exposed with a screen for 1 to 7 days.

RESULTS

Morphological characteristics of intracellular particles. To study the mechanism of M-MuLV $Pr65^{gag}$ transport and assembly, we initially used EM to visualize the effects of monensin treatment on virus-producing and non-virus-producing cells. Surprisingly, virus-producing cells showed intracellular particles, even in the absence of monensin (Fig. 1). Since these observations were unexpected for type C retrovirus assembly, we verified them by analysis of Psi2 cells, M-MuLV-infected 3T3 cells, and Psi2 cells expressing a retroviral vector. To exclude the possibility that intracellular particles represented endogenous type A particles, we analyzed two lines of NIH 3T3 fibroblasts in precisely the same manner and did not observe any virus particles in any of the fields from all the grids examined. In contrast, particles from virus-producing cells (Fig. 1) were roughly 120 nm in diameter and appeared to be immature, as judged from their electron density at the particle rim and the lack of a centrally located dense core. Many of the virions appeared within the RER (Fig. 1), but there also were those that appeared to be within vesicles. Interestingly, some particles appeared to be assembling into intracellular membranes (uppermost arrow in Fig. 1A). As an attempt to quantify our EM observations, we tabulated the numbers of virus particles at the plasma membrane or within intracellular compartments. Table 1 shows that 70 and 90% of the particles in 3T3-infected and Psi2 virus producer cells were intracellular; this is a maximum estimate, since released particles which do not remain cell associated are not counted. There was a significant difference between the two cell lines analyzed with respect to the location of intracellular virions. Particles were localized predominantly to RER, Golgi, and vesicle compartments of Psi2 cells, while the majority of particles in M-MuLV-infected 3T3 cells were located within vacuoles. The reason for this difference is unclear but could be caused by a general impairment of vesicular transport function in Psi2 cells (42).

To extend our observations, we also examined Psi2 cells by immunofluorescence light microscopy, using an antibody against the amino-terminal (p15) matrix domain of $Pr65^{gag}$ (Fig. 2). While this anti-p15 antibody (7) gave no signal on uninfected 3T3 cells (Fig. 2F), the cells exhibited fluorescence at the periphery of the cell and along cell projections (Fig. 2B and D), possibly indicative of assembly and release

FIG. 1. Electron micrographs showing intracellular M-MuLV particles. (A) A Psi2 cell with intracellular, assembled M-MuLV cores. Arrows denote particles which are assembling or within RER, Golgi, or vesicle compartments. (B) Large numbers of intracellular particles within a Psi2 retrovirus packaging cell which expresses a *neo* vector. Scale bars represent 1,000 nm.

of viral particles. Additionally, cells showed intense punctate fluorescence (Fig. 2B and D) surrounding the nuclei in the vicinity of the RER, consistent with the presence of intracellular particles within RER and/or Golgi compartments. We estimate the smallest resolvable spots of fluorescence to be 100 to 500 nm in diameter, and the smallest of these may represent individual virus particles. The distinct punctate pattern demonstrated by the $p15^{gag}$ antigen supports the notion that a significant proportion of intracellular Gag protein is not in monomeric form (see below).

Detergent resistance of intracellular particles. Having observed intracellular virus particles, we wanted to characterize their status of assembly and determine which components were within the particles. Since Gag proteins of type D intracellular particles are not solubilized by 0.5% Triton X-100 (32), we reasoned that we might be able to separate fully formed type C cores from monomeric $Pr65^{gag}$ protein by subcellular fractionation in the presence of Triton X-100. Such an approach could serve as biochemical support of our EM observations if $Pr65^{gag}$ were enriched in postnuclear Triton X-100-resistant pellets. Figure 3 shows subcellular fractionation results with three cell lines and the effects of

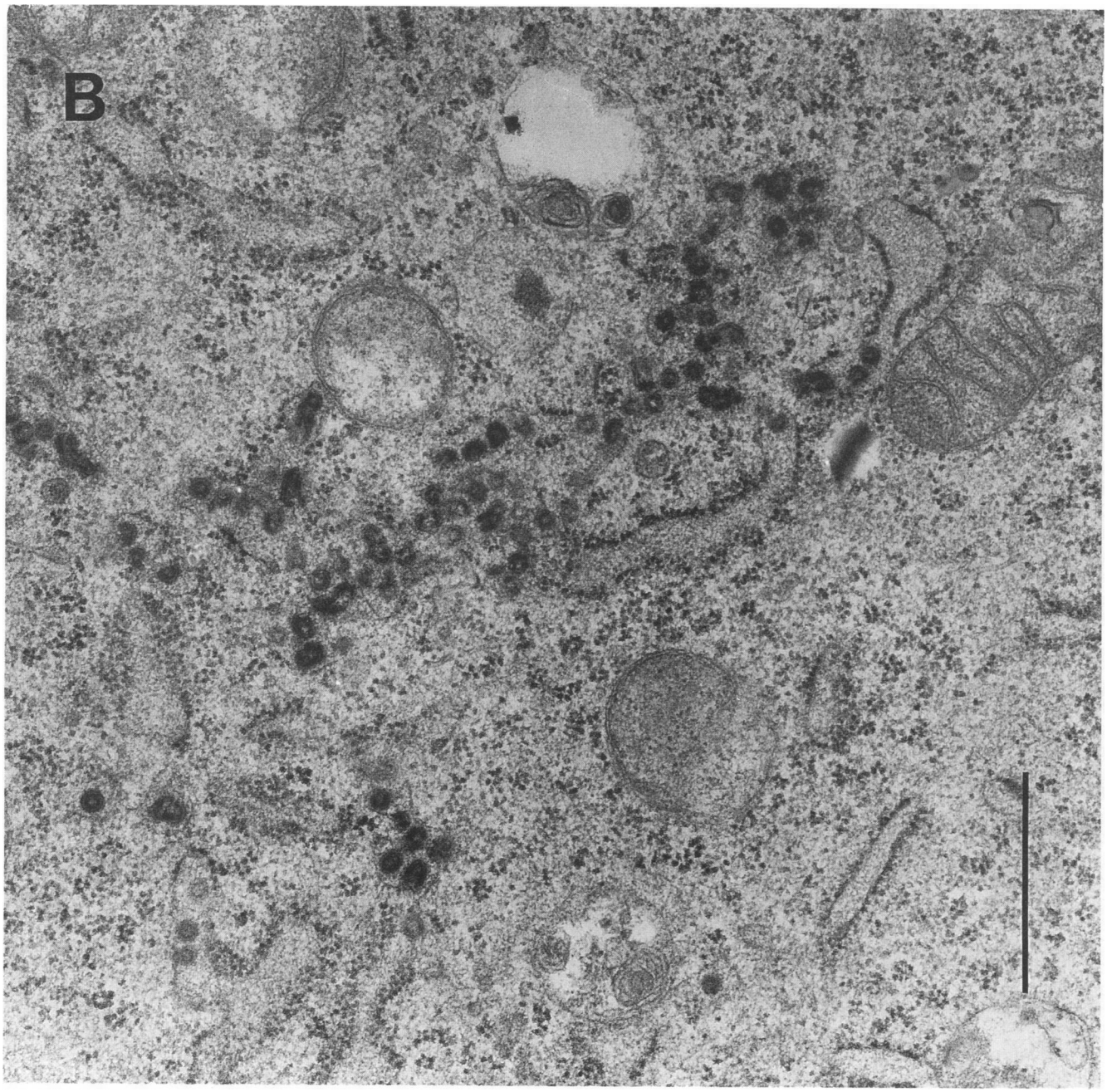

treatment of PNS with Triton X-100 prior to separating crude membranes (P2) from cytosol (S2). Not surprisingly, 3T3 cell lysates showed little or no reactivity to an anti-p12^{gag} (7) antibody (Fig. 3, lanes E to H). In contrast, Psi2 packaging cells (lanes A to D and M to T) and 3T3 cells chronically infected with M-MuLV (lanes I to L) showed three immunoreactive bands: Pr65^{gag}, p12^{gag}, and p27, which may be a Pr65^{gag} cleavage intermediate consisting of the M-MuLV matrix (p15) and p12 domains (16). In both Psi2 and M-MuLV-infected cells, unprocessed Pr65^{gag} appeared to be present in greater quantities than p12^{gag}, but in infected 3T3 cells, the p27^{gag} product appeared at roughly the same levels as Pr65^{gag}, whereas Psi2 Pr65^{gag} levels were greater than those of the putative intermediate; we have not determined the reason for this difference. Nevertheless, a consistent observation was that Pr65^{gag} was membrane associated in the absence of detergent (lanes A versus B and I versus J) and that addition of 0.5% Triton X-100 did not affect the Pr65^{gag} fractionation pattern (lanes C versus D and K versus L). One possible explanation for this fractionation pattern is that intracellular Pr65^{gag} may be bound in a nonionic detergent-resistant form to cytoskeletal elements (10, 11). To test this hypothesis, Psi2 cell PNS was treated with 600 mM NaCl, which reportedly eliminates cytoskeleton binding (10,

TABLE 1. EM localization of virus particles[a]

Cells	No. of total virions counted	No. of extracellular virions	No. of intracellular virions		No. of budding virions		% Intracellular virions
			In vacuoles	In RER	At plasma membrane	Intracellular	
Psi2	166	15	5	141	10	6	91
Infected 3T3	287	81	167	39	2	1	72

[a] Psi2 cells expressing the BAG retroviral vector, M-MuLV-infected 3T3 cells, and 3T3 cells were prepared for EM analysis as described in Materials and Methods. For tabulation of virus particles, sectioned cells were chosen solely by the criterion that they lay fully within one grid sector. No virus particles were observed in any of the fields of 3T3 cells examined. For both Psi2 and M-MuLV-infected 3T3 cell lines, 22 cells were completely examined for virus particle content. Total extracellular and intracellular particles were counted, and intracellular particles were distinguished as to whether they were within vacuoles or the RER, Golgi bodies, or vesicles. In each compartment, the number of budding particles was determined. Note that EM photography (Fig. 1) and tabulation of intracellular particles occurred on separate occasions.

11). However, while such treatment solubilized p27, it had a much smaller effect on the $Pr65^{gag}$ pattern (lanes O and P). Even when Psi2 PNS was treated sequentially with Triton X-100 and NaCl, a considerable amount of membrane-associated $Pr65^{gag}$ (approximately 25 to 50%) remained in the pellet fraction (lanes S and T). These results are consistent with the interpretation that at least a quarter of the intracellular $Pr65^{gag}$ protein tends to be present in a Triton X-100-resistant multimeric form. Furthermore, the appearance of a $Pr180^{gag\text{-}pol}$ band in Triton X-100 PNS pellets (evident when larger amounts of material were used; lanes R and T) suggests that *pol* gene products also are present in intracellular aggregates, an interpretation which is supported below.

To examine further the effects of Triton X-100 treatment on particles and demonstrate to what extent membrane proteins were solubilized, additional studies were performed. Figure 4 shows the effect of Triton X-100 treatment on the distribution patterns of several proteins in virus-producing cells expressing human PLAP which were subjected to subcellular fractionation protocols. As in Fig. 3, $Pr65^{gag}$ pelleted even in the presence of Triton X-100 (Fig. 4, lanes D versus C). However human PLAP, which localizes to the plasma membrane, and $gp70^{env}$, the mature proteolytic product of $Pr80^{env}$, were both predominantly in the pellet of untreated fractionation (lane B), while the addition of Triton X-100 shifted these proteins toward the supernatant fraction (lane C). $Pr80^{env}$, which is the RER and early Golgi M-MuLV Env protein form (40), was solubilized considerably by the detergent treatment (compare lanes C and A). This experiment shows that the detergent treatment had a much greater effect on membrane proteins than on $Pr65^{gag}$.

To confirm the effects of Triton X-100 treatment on cellular and viral proteins, we subjected two additional cell lines to subcellular fractionation with and without detergent treatment and assayed the contents of each fraction. The two cell lines expressed different enzymatically active GBG fusion proteins, both of which are transported to the plasma membrane and released from cells. However, only 5 to 20% of the GBG1560 fusion protein is incorporated into virions, while 50 to 80% of the GBG2051 protein enters virus particles (18). Table 2 shows the results of our fractionations with Psi2 packaging cells expressing the GBG1560 or GBG2051 protein. In agreement with our results from Fig. 4, the RER NADPH cytochrome *c* reductase and Golgi galactosyltransferase activities were solubilized two- to threefold by detergent treatments (compare activity percentages in treated versus untreated pellets in each experiment). Also, the GBG1560 protein, which assembles poorly into particles, is Triton X-100 solubilized; in contrast, the GBG2051 protein is relatively resistant to solubilization (Table 2). The data in Table 2, Fig. 3, and Fig. 4 indicate that up to half of the M-MuLV intracellular $Pr65^{gag}$ and GBG2051 proteins present were in Triton X-100-resistant forms. These results are consistent with our EM observations.

Characterization of intracellular particles. To examine whether viral RNA was associated with intracellular particles, we designed an experiment to ascertain whether viral RNA is enriched in pellet fractions of Triton X-100-treated PNS material. Our approach was to determine whether packageable RNA expressed from proviral retroviral vector constructs was enriched in Triton X-100-resistant pellets of virus-producing (Psi2) versus non-virus-producing (3T3) PNS. To do so, we used matched Psi2 and 3T3 cells expressing the *neo* gene from proviral constructs and assayed the subcellular distributions of viral *neo* transcripts and, as a control, cellularly derived rpL3 (28) transcripts by RNase protection assays (see Materials and Methods).

Figure 5a shows the results of an RNase protection assay using the rpL3 probe to analyze total RNA, mock-treated PNS pellet (P2) RNA, and Triton X-100-treated PNS pellet (Triton-P2) RNA of the Psi2 and 3T3 *neo*-expressing (Psi2-*neo* and 3T3-*neo*) cells. Lane I shows the probe alone without RNase treatment, lane H contained total cellular RNA from a positive control cell line, and lane G is a negative (tRNA) control. As shown in lanes C and D, for which total cellular RNA was used, the rpL3 transcript was expressed to similar levels in Psi2-*neo* and 3T3-*neo* cell lines. The P2 subcellular fractions (lanes A and B) also contained similar quantities of rpL3 transcript. Similarly, when the PNS was treated with 0.5% Triton X-100 prior to centrifugation, the Triton-P2 fractions from Psi2-*neo* (lane E) and 3T3-*neo* (lane F) cells contained roughly equivalent levels of rpL3 RNA. Note that while the rpL3 RNA is present in P2 (lanes A and B) and, to a lesser extent, Triton-P2 (lanes E and F) of Psi2-*neo* and 3T3-*neo* cells, these results can not be used as an absolute indicator of the subcellular localization patterns of the rpL3 transcript; this is because we found it difficult to assess transcript levels in nuclease-rich nuclear pellet and supernatant (S2) fractions. However, since the subcellular localization of rpL3 RNA was unaffected by virus production, it served as a control for cellular RNA levels within given P2 and Triton-P2 fractions.

Our results with packageable *neo* RNA in 3T3 and Psi2 cells are shown in Fig. 5b, where lane designations and fractions are identical to those in Fig. 5a. Lane I contained the *neo* probe alone without RNase treatment, lane H was the positive control, and lane G was the tRNA negative control. Total *neo* RNA levels in Psi2-*neo* and 3T3-*neo* cells are shown in lanes C and D, respectively. As shown, the levels of neo RNA were similar, but the 3T3 cells (lane D)

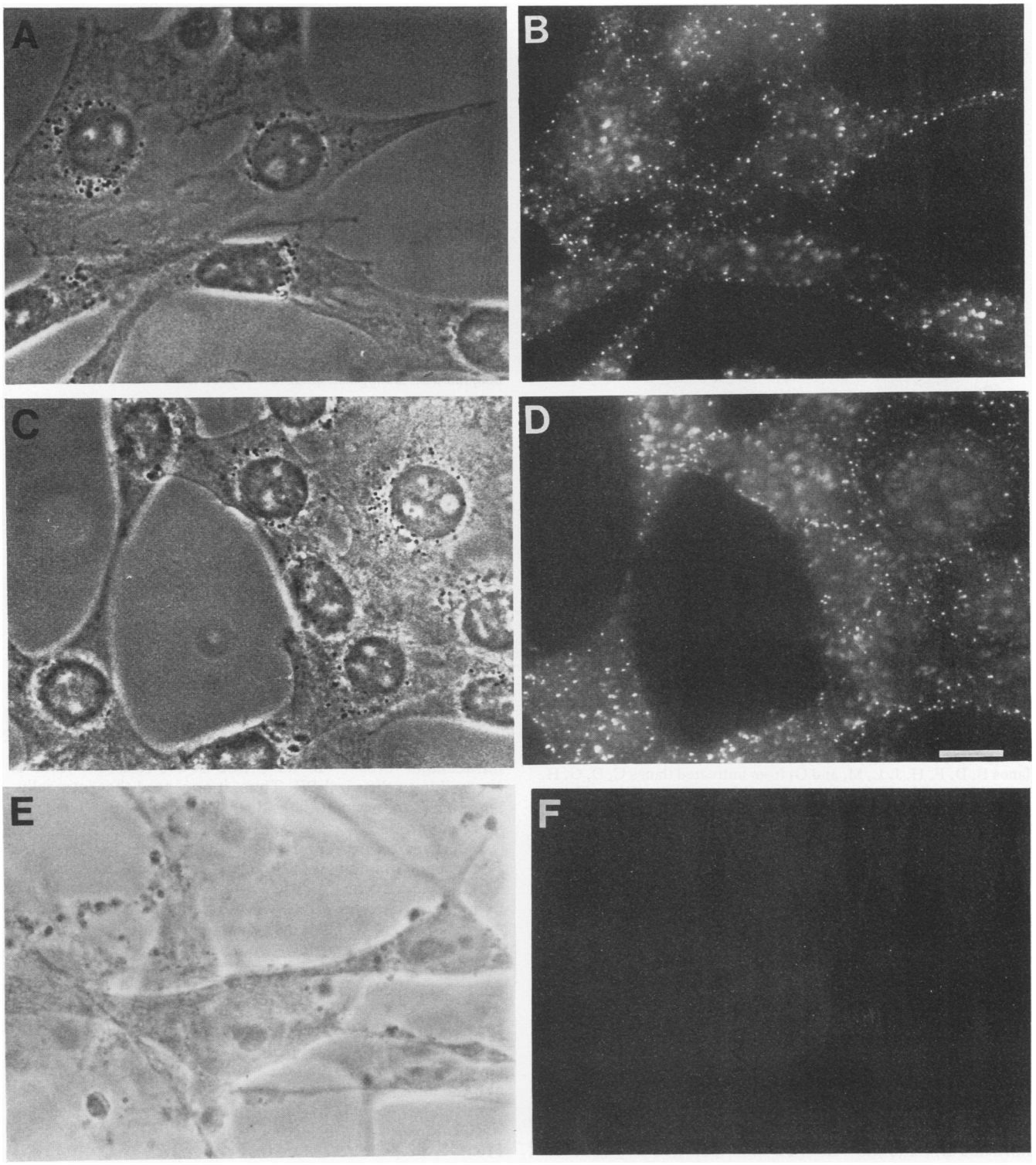

FIG. 2. Immunofluorescent localization of M-MuLV Gag proteins in Psi2 cells. Matched phase-contrast (A, C, and E) and anti-p15^{gag} immunofluorescence (B, D, and E) micrographs of Psi2 cells expressing the BAG retroviral vector (A to D) or negative control 3T3 fibroblast cells (E and F) are shown. For the negative control (F), photography exposure times and conditions were identical to those in panels B and D. As illustrated, the M-MuLV p15^{gag} antigen shows plasma membrane as well as perinuclear staining. The size bar in panel D represents 20 μm; we estimate the smallest resolvable immunofluorescent spots to be 100 to 500 nm.

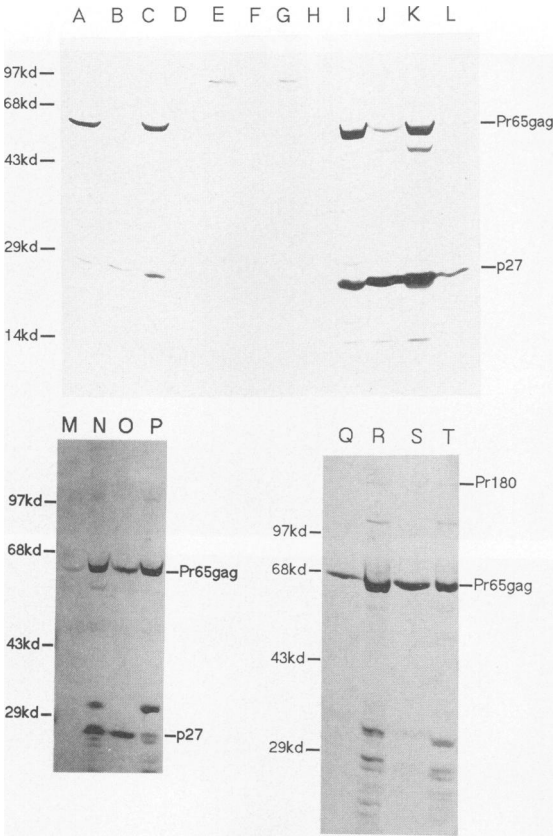

FIG. 3. Effect of Triton X-100 treatment on intracellular Gag fractionation. PNS fractions of Psi2 (lanes A to D and M to T), 3T3 (lanes E to H), and M-MuLV-infected 3T3 (lanes I to L) cells were electrophoresed and immunoblotted for detection of Pr65 and p12^{gag} proteins. Supernatants and pellets from PNS fractions were treated with and without 0.5% Triton X-100 or NaCl (600 mM, final concentration) and centrifuged for 15 min at 201,000 × g. Lanes were pellets (lanes A, C, E, G, I, K, N, and P) and supernatants (lanes B, D, F, H, J, L, M, and O) from untreated (lanes C, D, G, H, K, L, M, and N), NaCl-treated (lanes O and P), or Triton X-100-treated (lanes A, B, F, G, I, and J) PNS samples. In lanes Q to T, Triton X-100 pellets were resuspended by Dounce homogenization, mock treated (lanes Q and R) or treated with NaCl (lanes S and T), and fractionated again into supernatant (lanes Q and S) and pellet (lanes R and T) fractions. In all experiments, supernatant and pellet material represented 1/10 and 1/3 of the total respective supernatant and pellet samples. Pr65^{gag}, p12^{gag}, Pr180$^{gag\text{-}pol}$, and a proteolytic intermediate, p27, are indicated.

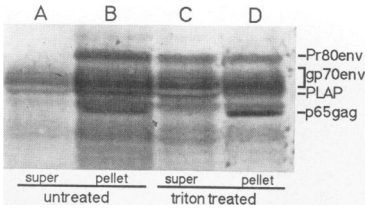

FIG. 4. Resistance of Pr65^{gag} to Triton X-100 solubilization. Psi2 virus-producing cells expressing human PLAP (22) were harvested and Dounce homogenized as described in Materials and Methods. PNS were treated with Triton X-100 or untreated. The samples were fractionated into soluble and insoluble fractions by centrifugation at 201,000 × g for 15 min at 4°C. Matching supernatants (10% of total sample) and pellets (25% of total sample) were subjected to SDS-polyacrylamide gel electrophoresis and electroblotted onto a nitrocellulose filter. Pr65^{gag}, PLAP, and M-MuLV Pr80^{env} and gp70^{env} were detected by sequential antibody binding and color reaction steps. Protein bands are as indicated. Lanes: A and B, untreated supernatant and pellet samples; C and D, Triton X-100-treated supernatant and pellet samples. Note that only part of the gel is magnified to distinguish each of the proteins.

expressed slightly more than the infected Psi2 cells did (lane C). The P2 fractions (lanes A and B) both contained *neo* transcript, with the Psi2 cells having slightly higher levels; this result suggested that the presence of virus particles might enrich packageable RNA to the P2. Such an interpretation was supported by results on RNA from Triton-P2 fractions; i.e., Psi2-derived cells contained significantly more *neo* RNA in the Triton-P2 than their 3T3-neo counterparts did. This difference indicates that *neo* transcript fractionation was dependent on the expression of the Psi2 genome and implies that viral RNA is associated with intracellular particles.

As shown in Fig. 3 (lanes R and T), the Gag-Pol protein precursor Pr180$^{gag\text{-}pol}$ appeared enriched in the Triton-X P2 fraction, suggesting that Gag-Pol proteins become associated with intracellular Gag protein complexes. However, as an independent attempt to determine whether *pol* gene products were incorporated into intracellular particles, we initially attempted reverse transcriptase assays but were hampered by high background activity levels in subcellular compartments. However, we next examined the potential presence of the *pol* gene PR product in intracellular particles. For these experiments, Psi2 PNS, containing Pr65^{gag} exclusively in a Triton X-100-resistant form (Fig. 3 and 4), was isolated and incubated at 37°C for 0, 30, 60, or 120 min to monitor PR-mediated cleavage of Pr65^{gag}. As illustrated in Fig. 6 (lanes A to D), during such a time course, Pr65^{gag} decreased with a concomitant increase in p30^{gag} levels. In contrast, Pr65^{gag} in the PNS from the viral PR-deficient cell line TR291F did not become converted to p30 during incubations (Fig. 6, lanes E to H). These results suggested that Psi2 intracellular Pr65^{gag} in its Triton X-100-resistant form is accessible to the viral PR. Thus, it appeared that intracellular particles contain both viral RNA (Fig. 5) and at least one *pol* gene product.

Detergent treatment of extracellular M-MuLV particles. Because we assumed that, like type D intracellular particles (32), immature type C particles were resistant to dissociation by nonionic detergents, we wished to verify this notion with extracellular M-MuLV particles. To do so, we isolated extracellular virus particles, incubated them in the absence or presence of detergent, and separated supernatant from pellet material after centrifugation at 150,000 × g (65,000 rpm on a Beckman TLA-100 rotor) for 15 min at 4°C. Figure 7 shows the results of such an experiment after electrophoresis and immunoblotting of supernatants and pellets to detect Gag proteins. In untreated samples, both processed p30^{gag} and the small amount of Pr65^{gag} were confined to the pellet (lanes B versus A). In contrast, in the presence of Triton X-100 (lanes C, D, G, and H) or NP-40 (lanes E and F), Pr65^{gag} still pelleted (lanes D, F, and H), while p30^{gag} was solubilized (lanes C, E, and G). Similar results were obtained with virus from M-MuLV-infected 3T3 cells and from M-MuLV PR mutant-expressing TR291F cells (19). In all experiments, Pr65^{gag} pelleted in the presence of nonionic detergent, while p30^{gag} was solubilized. This result implied that processed p30^{gag} and Pr65^{gag} were not present in the same virus particles or that conversion from a completely

TABLE 2. Fractionation of untreated and Triton X-100-treated cell lysates[a]

Psi2 cells expressing:	Marker	Untreated cells			Treated cells		
		Pellet	Supernatant	% in pellet	Pellet	Supernatant	% in pellet
GBG1560	Total protein (μg)	270	700	28	260	750	26
	Galactosyltransferase (cpm)	2,209	770	74	1,104	3,806	22
	NADPH cytochrome *c* reductase (U)	388	204	66	138	548	20
	β-Galactosidase (U)	21.2	2.7	89	6.2	18.6	25
GBG2051	Total protein (μg)	270	650	29	240	900	21
	NADPH cytochrome *c* reductase (U)	224	142	61	120	344	26
	β-galactosidase (U)	12.0	5.6	68	9.1	8.1	53

[a] Pellets or supernatants from untreated or Triton X-100-treated PNS of Psi2 cells (2×10^7 per experiment) expressing GBG fusion proteins were obtained as described in Materials and Methods. As described previously (18), the GBG1560 protein is released from cells in a low-density fraction but is not efficiently incorporated into virions, while the GBG2051 protein is incorporated efficiently into virions. Pellet and supernatant fractions were assayed for total protein, galactosyltransferase activity (a Golgi marker), NADPH cytochrome *c* reductase activity (an RER marker; 1 U = [(change in absorbance × 1,000]/min), and β-galactosidase activity. Values shown reflect the total calculated amount in each sample.

immature to completely mature particle must be very rapid after the initial cleavages occur. To distinguish between these possibilities, we examined early collections of virus particles from Psi2 cells. At our earliest time points (less than 2 h), the major portion of virus particle-associated *gag* antigen in medium supernatants was present in the mature form. Significantly, particle-associated medium $Pr65^{gag}$ did not become converted to the mature form over a 10-h, 37°C incubation (data not shown). These results suggest that if a particle is released in the immature form, it remains so. This result contrasts with those from intracellular particles (Fig. 6, lanes A to D), a difference that is discussed below.

DISCUSSION

By EM of virus-producing cells, we observed M-MuLV virions assembling on intracellular membranes within infected cells. EM analysis of M-MuLV-infected and virus particle-packaging Psi2 cells, but not of several different 3T3 lines, showed that particles can assemble on and bud through intracellular membranes. The results in Table 1 showed that although both Psi2 and M-MuLV-infected 3T3 cells contained intracellular particles, the infected 3T3 line has a very high percentage of vacuole-associated virus rather than RER, Golgi, and vesicle particles. While we have no data which clarify this difference, it is possible that a slight impairment of vesicular transport processes in either of the cell lines might account for this variability. Our immunofluorescence microscopy results also suggested that M-MuLV Gag proteins may assemble intracellularly into higher-order structures. This interpretation was suggested by the punctate quality of p15 staining rather than the haze of fluorescence expected for nonaggregated cytoplasmic antigens. We believe that these intracellular particles represent assembling structures rather than infecting virions for several reasons. First, infection of cells by ecotropic retroviruses should be inhibited by receptor interference (40). Second, intracellular particles appeared to be immature (Fig. 1), which is not consistent with infection by mature extracellular virions. Finally, several of the particles depicted in the micrographs (Fig. 1) appeared to be assembling onto intracellular membranes.

Biochemical studies support the notion that M-MuLV particles were formed within Psi2 and M-MuLV-infected cells. Most of the intracellular Gag protein in these cells consisted of the precursor $Pr65^{gag}$; using a modification of

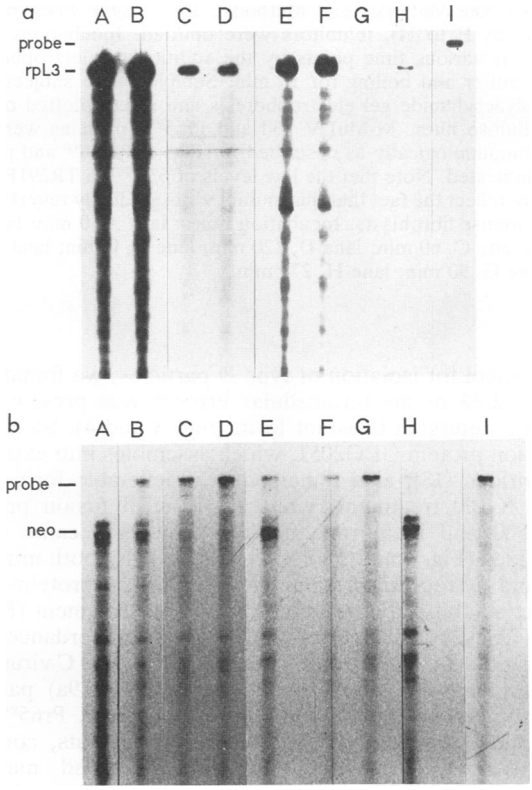

FIG. 5. Viral RNA content of untreated and Triton X-100-treated pellet fractions. (a) rpL3-labeled antisense RNA was prepared and used to detect rpL3 transcript by RNase protection in various samples as described in Materials and Methods. Psi2 virus-producing cells expressing a packageable neomycin-transducing retroviral vector (lanes A, C, and E) and 3T3 cells expressing the *neo* vector (lanes B, D, and F) were analyzed for the presence of the cellular rpL3 transcript in PNS pellet RNA (lanes A and B), total cellular RNA (lanes C and D), and Triton X-100-treated PNS pellet RNA (lanes E and F). Lanes G, H, I contain negative control (tRNA), positive control, and undigested probe samples, respectively. Note that rpL3 RNA levels in pellet fractions are used to normalize for the nonspecific cellular RNA content of total cellular and pellet fractions. (b) *neo*-labeled antisense RNA was used to detect *neo* transcript. Lane designations and procedures are identical to those in panel a. Note that film processor roller marks are evident and that only a portion of the gel is magnified to show the largest protected bands.

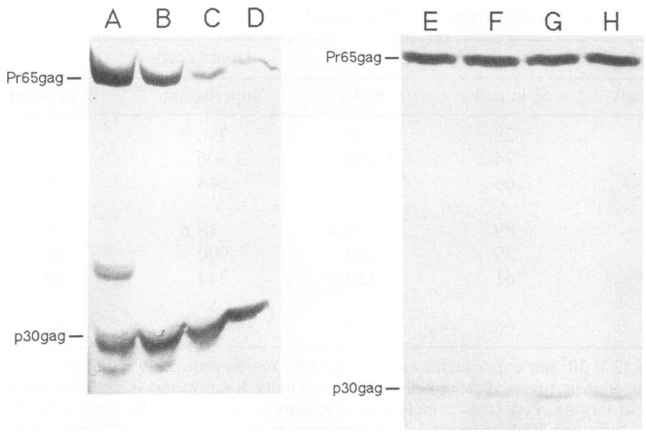

FIG. 6. Proteolysis of $Pr65^{gag}$ in Psi2 PNS. Psi2 cell (lanes A to D) or M-MuLV PR-deficient TR291F cell (lanes E to H) PNS were incubated at 37°C in time course studies of $Pr65^{gag}$ proteolysis. With Psi2 PNS (lanes A to D), lysates contained a cocktail of protease inhibitors (see Materials and Methods); for TR291F PNS incubations (lanes E to H), inhibitors were omitted. Incubations were stopped at various time points by the addition of electrophoresis sample buffer and boiling for 10 min. Samples were subjected to SDS-polyacrylamide gel electrophoresis and electroblotted onto a nitrocellulose filter. M-MuLV p30 and $Pr65^{gag}$ proteins were detected immunologically as described for Fig. 4. $Pr65^{gag}$ and $p30^{gag}$ are as indicated. Note that the low levels of $p30^{gag}$ in TR291F cells probably reflect the fact that this mutant virus gradually reverts over time in mouse fibroblasts. Incubation times: lane A, 0 min; lane B, 30 min; lane C, 60 min; lane D, 120 min; lane E, 0 min; lane F, 30 min; lane G, 90 min; lane H, 270 min.

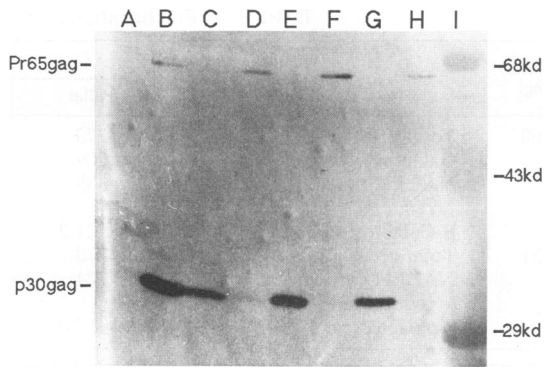

FIG. 7. Detergent sensitivity of extracellular virions. Psi2 extracellular virions, enriched by purification, were treated with detergents and centrifuged to examine the difference in protein interactions in immature versus mature virions. Matching supernatants (16% of the total sample; lanes A, C, E, and G) and pellets (50% of the total sample; lanes B, D, F, and H) were obtained by centrifugation at 150,000 × *g* (65,000 rpm on a TLA-100 rotor) for 15 min at 4°C after mock treatment (lanes A and B), 0.1% Triton X-100 treatment (lanes C and D), 0.1% NP-40 treatment (lanes E and F), or 0.1% Triton X-100–100 mM dithiothreitol treatment. Gag proteins in samples were detected with an anti-p30 antibody after electrophoresis and electroblotting. Marker protein sizes, indicated on the right, are from marker proteins in lane I.

the protocol for isolation of type D particles, we found that at least 25% of the intracellular $Pr65^{gag}$ was present in a nonionic detergent-resistant form (Fig. 3 and 4). Similarly, the fusion protein GBG2051, which assembles into extracellular virions (18), also remained in a pelletable form after Triton X-100 treatment, while the control fusion protein GBG1560 and membrane marker proteins became more solubilized (Fig. 4 and Table 2). Interestingly, both intracellular and extracellular mature M-MuLV Gag proteins also became solubilized on nonionic detergent treatment (Fig. 3 and 7). These results with M-MuLV are in concordance with observations on mature and immature avian type C virus (38) and human immunodeficiency virus (HIV) (39a) particle sensitivities. Additionally, the fractionation of $Pr65^{gag}$ to Triton pellets and $p30^{gag}$ to Triton supernatants, coupled with the observation that particle-associated medium $Pr65^{gag}$ does not become processed in a 10-h incubation (data not shown), suggests that extracellular immature particles may be PR defective (Fig. 7). This result is in contrast with our observations of intracellular particles, which appear to possess PR activity (Fig. 6). Such a difference may result from the absence of *pol* gene products in extracellular immature particles, which would imply that ordinarily, a very small number of Gag-Pol proteins enter virions. Alternatively, the disparity in extracellular versus intracellular particle processing of $Pr65^{gag}$ might be due to an as yet undetermined structure or cofactor difference between the two immature forms.

We do not know the amount of $Pr65^{gag}$ oligomerization necessary to confer resistance to Triton X-100 solubilization. However, from the clearing rates during one centrifugation step, we estimate that the predominant intracellular form of Triton X-100-resistant $Pr65^{gag}$ is in a complex, or complexes, of greater than 165S. Furthermore, from our electron micrographs (Fig. 1), we assume that the intracellular particles are lipidated, although we have no direct evidence showing this. Also unclear for methodological reasons is whether the M-MuLV Env protein is associated with intracellular particles. However, both viral RNA (Fig. 5) and PR (Fig. 6) appear to be associated with intracellular $Pr65^{gag}$.

We do not claim that intracellular assembly of M-MuLV particles is the natural route of virus assembly, yet our observations shed some light on the process. In particular, models of type C retrovirus assembly often involve a critical role for the plasma membrane, possibly by virtue of a specific membrane binding interaction. Our results necessitate a qualification of such a model. In this regard, we note that intracellular particles have been observed with other type C retrovirus-infected cells (3) and that HIV particle assembly can occur in murine and insect cells (13, 39a). Thus, there is no absolute species or subcellular membrane specificity to the process; assembly on membranes conceivably could be nucleated by a specific receptor, but such a receptor is not absolutely membrane or species specific.

What determines the incidence of intracellular versus cell surface assembly of type C viruses? By our simplest model, the determining factor may be the rate of Gag transport. We have proposed that a high proportion of cotranslationally myristylated Gag proteins bind to the cytoplasmic faces of intracellular membranes and travel in association with vesicles to the cell surface (16, 18). Presumably, concentration of Pr65 in two dimensions at the plasma membrane achieves a high enough accumulation of monomers for virion formation. If this is the case, then perturbation of Gag transport should result in its increased accumulation on intracellular membranes and the formation of intracellular particles. Possibly with HIV, a protein such as Vpu (39) may be required to counteract this effect under certain circumstances.

A functional role, if any, for internally formed particles in

virus infections is unclear. At one extreme, it could be a viable and frequently used pathway for the elaboration of infectious virions. However, retrovirus assembly undeniably can occur at the plasma membrane, as evidenced in numerous EM studies (36, 38, 41). Additionally, virion assembly by an internal route would require Env protein association at the RER as well as transport of the enveloped particle through the lumenal compartments of the RER and Golgi compartment to the cell surface. Nevertheless, we do not consider intracellular particles to represent a complete dead end, since our studies suggest that a small percentage of them may be infectious (data not shown). As suggested for HIV infections (24), intracellular particles could constitute a reservoir of virus during the progression of disease.

ACKNOWLEDGMENTS

This work could not have been started without the assistance and guidance of Paula Stenberg. We also are grateful to David Kabat, Chin-tien Wang, Sam Whiting, and Milton Yatvin for helpful advice and stimulating discussion. The TR291F cell line and a negative control 3T3 cell line were generously provided by Alan Rein; anti-M-M-MuLV Gag hybridoma cell lines were the kind gift of Bruce Chesebro.

Our research was made possible by grant 1-FY91-0049 from the March of Dimes Birth Defects Foundation and by grant 2 R01CA47088-04 from the National Cancer Institute.

REFERENCES

1. **Barklis, E., R. Mulligan, and R. Jaenisch.** 1986. Chromosomal position of viral mutation permits retrovirus expression in embryonal carcinoma cells. Cell **47**:391–399.
2. **Bolognesi, D., R. Montelaro, H. Frank, and W. Schafer.** 1978. Assembly of type C oncoronaviruses: a model. Science **199**: 183–186.
3. **Bosch, J., and R. Schwarz.** 1984. Processing of $gPr92^{env}$, the precursor to the glycoproteins of Rous sarcoma virus: use of inhibitors of oligosaccharide trimming and glycoprotein transport. Virology **132**:95–109.
4. **Bradford, M. M.** 1976. A rapid and sensitive method for the quantitation of protein utilizing the principle of protein-dye binding. Anal. Biochem. **72**:248–254.
5. **Bretz, R., H. Bretz, and G. E. Palade.** 1980. Distribution of terminal glycosyltransferases in hepatic golgi fractions. J. Cell Biol. **84**:87–101.
6. **Cepko, C., B. Roberts, and R. Mulligan.** 1984. Construction and applications of a highly transmissible murine retrovirus shuttle vector. Cell **37**:1053–1062.
7. **Chesebro, B., W. Britt, L. Evans, K. Wehrly, J. Nishio, and M. Cloyd.** 1983. Characterization of monoclonal antibodies reactive with murine leukemia viruses: use in analysis of strains of Friend MCF and Friend ecotropic murine leukemia virus. Virology **127**:134–148.
8. **Chirgwin, J., A. Przybyla, R. MacDonald, and W. Rutter.** 1979. Isolation of biologically active ribonucleic acid from sources enriched in ribonuclease. Biochemistry **18**:5294–5299.
9. **Dickson, C., and M. Atterwill.** 1980. Structure and processing of the mouse mammary tumor virus glycoprotein precursor $Pr73^{env}$. J. Virol. **35**:349–361.
10. **Edbauer, C., and R. Naso.** 1983. Cytoskeleton-associated $Pr65^{gag}$ and retrovirus assembly. Virology **130**:415–426.
11. **Edbauer, C., and R. Naso.** 1984. Cytoskeleton-associated $Pr65^{gag}$ and assembly of retrovirus temperature-sensitive mutants in chronically infected cells. Virology **134**:389–397.
12. **Gething, M., K. McCammon, and J. Sambrook.** 1986. Expression of wild-type and mutant forms of influenza hemagglutinin: the role of folding in intracellular transport. Cell **46**:939–950.
13. **Gheysen, D., E. Jacobs, F. de Foresta, C. Thiriart, M. Francotte, D. Thines, and M. De Wilde.** 1989. Assembly and release of HIV-1 precursor Pr55 gag virus like particles from recombinant baculovirus-infected insect cells. Cell **59**:103–112.
14. **Gorelick, R., L. Henderson, J. Hanser, and A. Rein.** 1988. Point mutants of Moloney murine leukemia virus that fail to package viral RNA: evidence for a specific RNA recognition by a "zinc finger-like" protein sequence. Proc. Natl. Acad. Sci. USA **85**:8420–8424.
15. **Hanafusa, H., D. Baltimore, D. Smoler, K. Watson, A. Yaniv, and S. Spiegelman.** 1972. Absence of polymerase protein in virions of alpha-type Rous sarcoma virus. Science **177**:1188–1191.
16. **Hansen, M., L. Jelinek, S. Whiting, and E. Barklis.** 1990. Transport and assembly of Gag proteins into Moloney murine leukemia virus. J. Virol. **64**:5306–5316.
17. **Hendersen, L., H. Krutzsch, and S. Oroszlan.** 1983. Myristyl amino-terminal acylation of murine retroviral proteins: an unusual post-translational protein modification. Proc. Natl. Acad. Sci. USA **80**:339–343.
18. **Jones, T., G. Blaug, M. Hansen, and E. Barklis.** 1990. Assembly of Gag–β-galactosidase proteins into retrovirus particles. J. Virol. **64**:2265–2279.
19. **Katoh, I., Y. Yoshinaka, A. Rein, M. Shibuya, T. Odaka, and S. Oroszlan.** 1985. Murine leukemia virus maturation: protease region required for conversion from immature to mature core form and for virus infectivity. Virology **145**:280–292.
20. **Laemmli, U. K.** 1970. Cleavage of structural proteins during assembly of the head of bacteriophage T4. Nature (London) **227**:680–685.
21. **Levin, J. G., P. M. Grimley, J. M. Ramseur, and I. K. Berezesky.** 1974. Deficiency of 60 to 70S RNA in murine leukemia virus particles assembled in cells treated with actinomycin D. J. Virol. **14**:152–161.
22. **Mace, M. C., M. Hansen, S. Whiting, C. Wang, and E. Barklis.** 1992. Retroviral envelope fusions to secreted and membrane markers. Virology **188**:869–874.
23. **Mann, R., R. Mulligan, and D. Baltimore.** 1983. Construction of a retrovirus packaging mutant and its use to produce helper-free defective retrovirus. Cell **33**:153–159.
24. **Meltzer, M., D. Skillman, P. Gomatos, D. Kalter, and H. Gendelman.** 1990. Role of mononuclear phagocytes in the pathogenesis of human immunodeficiency virus infection. Annu. Rev. Immunol. **8**:169–194.
25. **Miller, A., and C. Buttimore.** 1986. Redesign of retrovirus packaging cell lines to avoid recombination leading to helper virus production. Mol. Cell. Biol. **6**:2895–2902.
26. **Norton, P., and J. Coffin.** 1985. Bacterial β-galactosidase as a marker of Rous sarcoma virus gene expression and replication. Mol. Cell. Biol. **5**:281–290.
27. **Omura, T., P. Siekevitz, and G. Palade.** 1967. Turnover of constituents of the endoplasmic reticulum membranes of rat hepatocytes. J. Biol. Chem. **242**:2389–2396.
28. **Peckham, I., S. Sobel, J. Comer, R. Jaenisch, and E. Barklis.** 1991. Retrovirus activation in embryonal carcinoma cells by cellular promoters. Genes Dev. **3**:2062–2071.
29. **Reik, W., H. Weiher, and R. Jaenisch.** 1985. Replication-competent M-MuLV carrying a bacterial suppressor tRNA gene: selective cloning of proviral and flanking host sequences. Proc. Natl. Acad. Sci. USA **82**:1141–1145.
30. **Rein, A., M. McClure, N. Rice, R. Luftig, and A. Schultz.** 1986. Myristylation site in Pr65gag is essential for virus particle formation by Moloney murine leukemia virus. Proc. Natl. Acad. Sci. USA **83**:7246–7250.
31. **Resh, M.** 1989. Specific and saturable binding of $pp60^{v\text{-}src}$ to plasma membranes: evidence for a myristyl-src receptor. Cell **58**:281–286.
32. **Rhee, S., and E. Hunter.** 1987. Myristylation is required for intracellular transport but not for assembly of D-type retrovirus capsids. J. Virol **61**:1045–1053.
33. **Rhee, S., and E. Hunter.** 1990. Structural role of the matrix protein of type D retroviruses in Gag polyprotein stability and capsid assembly. J. Virol. **64**:4383–4389.
34. **Rhee, S., and E. Hunter.** 1990. A single amino acid substitution within the matrix protein of a type D retrovirus converts its morphogenesis to that of a type C retrovirus. Cell **63**:77–86.
35. **Rose, J., and J. Bergmann.** 1983. Altered cytoplasmic domains affect intracellular transport of the vesicular stomatitis virus

glycoprotein. Cell **34**:513–524.
36. **Roth, M., R. Srinivas, and R. Compans.** 1983. Basolateral maturation of retroviruses in polarized epithelial cells. J. Virol. **45**:1065–1073.
37. **Shields, A., O. Witte, E. Rothenberg, and D. Baltimore.** 1978. High frequency of aberrant expression of Moloney murine leukemia virus in clonal infections. Cell **14**:601–609.
38. **Stewart, L., G. Schatz, and V. Vogt.** 1990. Properties of avian retrovirus particles defective in viral protease. J. Virol. **64**:5076–5092.
39. **Strebel, K., T. Klimkait, F. Maldarelli, and M. A. Martin.** 1989. Molecular and biochemical analyses of human immunodeficiency virus type 1 *vpu* protein. J. Virol. **63**:3784–3791.
39a. **Wang, C., and E. Barklis.** Unpublished data.
40. **Weiss, R., N. Teich, H. Varmus, and J. Coffin (ed.).** 1984. RNA tumor viruses, 2nd ed. Cold Spring Harbor Laboratory, Cold Spring Harbor, N.Y.
41. **Witte, O., and D. Baltimore.** 1978. Relationship of retrovirus polyprotein cleavages to virion maturation studied with temperature-sensitive murine leukemia virus mutants. J. Virol. **26**:750–761.
42. **Yatvin, M.** Personal communication.